



# Vapour-liquid equilibria in pure N-Methyl-1,3-diaminopropane (MAPA), 1,3-diaminopropane (DAP), 2-(Isopropylamino)ethanol (IPAE), *N*-tert-Butyldiethanolamine (N-TBDEA) and their aqueous solutions



Anastasia A. Trollebø, Ardi Hartono, Muhammad Usman, Muhammad Saeed, Hallvard F. Svendsen\*

Department of Chemical Engineering, Norwegian University of Science and Technology, NO-7491 Trondheim, Norway

## ARTICLE INFO

### Article history:

Received 6 March 2019

Received in revised form 16 September 2019

Accepted 20 September 2019

Available online 21 September 2019

### Keywords:

Vapour-liquid equilibrium

Pure amines

Aqueous solutions

NRTL

## ABSTRACT

New energy effective solvents are in demand to make global CO<sub>2</sub> capture feasible. Phase change solvents seem to be one avenue to reach this goal. This paper presents new experimental data and modelling results for four amines that have potential as new solvents in blends for post combustion CO<sub>2</sub> capture. Both pure component data and data for amine-water solutions, based on ebulliometer measurements, are presented. The data were fitted to an Antoine equation and an NRTL model in two ways: first in a combined fit of both pure component and binary data and then in separate fits to the individual data sets. The methods were compared and guidelines as to which method to use, based on available data, is provided. Data for 2-(Isopropylamino)ethanol (IPAE), *N*-tert-Butyldiethanolamine (N-TBDEA), *N*-Methyl-1,3-diaminopropane (MAPA) and 1,3-diaminopropane (DAP) from the literature were collected and compared with the new data sets.

All data and model parameters are given. For all amines, the best fits provided good to excellent representations of the available data.

© 2019 The Authors. Published by Elsevier Ltd. This is an open access article under the CC BY-NC-ND license (<http://creativecommons.org/licenses/by-nc-nd/4.0/>).

## 1. Introduction

In the struggle to mitigate global warming, CO<sub>2</sub> capture and storage is the only technology available to reduce the atmospheric CO<sub>2</sub> content. Capture by absorption is presently the most mature technology and the search for more energy efficient solvents is ongoing [1,2]. A promising approach is the combination of one primary and one tertiary or secondary amine, operating in an intermediate loading range. Thereby one may retain the fast absorption provided by the primary amine with, at least partially, the lower heat of absorption and ease of stripping of the tertiary or secondary amines. In addition, some of the amines have a potential for forming two liquid phases upon CO<sub>2</sub> loading, so-called phase change solvent systems.

This paper provides new pure component and binary aqueous solution VLE data for four amines: 1,3-diaminopropane (DAP), 2-(Isopropylamino)ethanol (IPAE), *N*-tert-Butyldiethanolamine (N-TBDEA) and *N*-Methyl-1,3-diaminopropane (MAPA) and compares this to existing literature data. Part of the data for DAP and

N-TBDEA were reported in anonymized form in Trollebø, *et al.* [3] as shown in the appended tables. The pure component and binary VLE data are fitted both individually and combined to an Antoine equation and an NRTL model.

Further, the paper provides new pure component density data for the four amines and compares the currently obtained data on density of pure MAPA, DAP and IPAE with literature data [4–11].

These amines were chosen for VLE testing because they were found to be promising alternatives to the classical MEA based CO<sub>2</sub> absorption process [12]. Basic data on pure component and binary amine/water systems form the basis for the development of equilibrium models for CO<sub>2</sub> loaded systems and mixed amine systems.

## 2. Theoretical background

### 2.1. Vapour-liquid equilibrium of pure compounds

The Antoine equation [13] is used to describe the  $P^{\text{sat}}-T$  dependencies of non-ideal gases also at higher pressures and temperatures, see Eq. (1).

\* Corresponding author.

E-mail address: [hallvard.svendsen@ntnu.no](mailto:hallvard.svendsen@ntnu.no) (H.F. Svendsen).

$$p^{\text{sat}} = 10^{(A + \frac{B}{T+C})} \quad (1)$$

where  $p^{\text{sat}}$  is saturation pressure (kPa),  $T$  is temperature (K) and  $A$ ,  $B$ ,  $C$  are constant parameters.

The Antoine equation was used in this work for description of the experimental  $p^{\text{sat}}-T$  curves.

## 2.2. Vapour-liquid equilibrium of binary systems

### 2.2.1. NRTL model

There exist several models that can be applied to binary systems to represent VLE curves and to calculate activity coefficients of compounds and excess Gibbs energy. Wilson [14] and Chen and Evans [15] used the concept of local compositions for calculations of excess Gibbs energy. Renon and Prausnitz [16] derived the NRTL (Non-random two liquid) model also based on the idea of local composition. Unlike the Wilson equation, which cannot be applied to immiscible mixtures, the NRTL equation is applicable to both completely miscible and partially miscible solutions and can be used for description of liquid-liquid systems. In this work, the NRTL model was used for the binary mixtures. The NRTL equation for excess Gibbs energy is:

$$\frac{G^E}{R \cdot T} = x_1 \cdot x_2 \left[ \frac{\tau_{21} \cdot G_{21}}{x_1 + x_2 \cdot G_{21}} + \frac{\tau_{12} \cdot G_{12}}{x_2 + x_1 \cdot G_{12}} \right] \quad (2)$$

where

$$\tau_{ij} = \frac{g_{ij} - g_{jj}}{R \cdot T}$$

$$G_{ij} = \exp(-\alpha \cdot \tau_{ij})$$

$$g_{ij} - g_{jj} = A_{ij} + B_{ij} \cdot (T - 273.15)$$

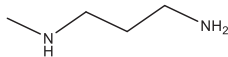
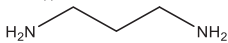
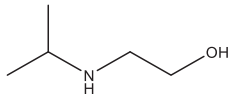
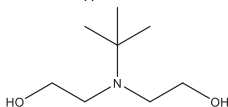
The NRTL equation contains five parameters, the  $A_{ij}$ ,  $B_{ij}$  and  $\alpha$ . Renon and Prausnitz [16] proposed estimation rules for the fifth parameter (non-randomness factor) according to the constituents of the system. In this work all five parameters were fitted to the data.

Activity coefficients can be calculated from the NRTL model as:

$$\ln \gamma_1 = x_2^2 \cdot \left[ \tau_{21} \cdot \left( \frac{G_{21}}{x_1 + x_2 \cdot G_{21}} \right)^2 + \frac{\tau_{12} \cdot G_{12}}{(x_2 + x_1 \cdot G_{12})^2} \right] \quad (3)$$

$$\ln \gamma_2 = x_1^2 \cdot \left[ \tau_{12} \cdot \left( \frac{G_{12}}{x_2 + x_1 \cdot G_{12}} \right)^2 + \frac{\tau_{21} \cdot G_{21}}{(x_1 + x_2 \cdot G_{21})^2} \right] \quad (4)$$

**Table 1**  
Amines used for measurements.

Amine	Abbreviation	CAS <sup>a</sup> number	Purity <sup>b</sup>	Molecular structure	Supplier
<i>N</i> -Methyl-1,3-diaminopropane	MAPA	6291-84-5	≥0.992		Sigma Aldrich
1,3-diaminopropane	DAP	109-76-2	≥0.999		Sigma Aldrich
2-(Isopropylamino)ethanol	IPAE	109-56-8	≥0.991		TCI
<i>N</i> -tert-Butyldiethanolamine	N-TBDEA	2160-93-2	≥0.999		Sigma Aldrich

<sup>a</sup> CAS No.: Chemical Abstract Service Register Number.

<sup>b</sup> in mass fraction taken from the Certificate of Analysis (COA). For MAPA, the water content was given as 0.0011 mass fraction. No water content data for the other components were given.

## 3. Materials and experimental setups

### 3.1. Materials

The amines used in this work are listed in Table 1.

Purities of supplied chemicals are specified in Table 1. All chemicals were used without additional purification. The water content of MAPA was given as a mass fraction of 0.0011. No water content data for the other components were given and we did not analyse for water in this work. Earlier, tests have been run in our laboratory on changes in amine concentration upon storage. We measured amine content in fresh amine and then again after experimentation, usually after a few days. The changes measured were below 0.1 wt%.

All solutions were prepared with deionized water. Aqueous blends of the amines were prepared based on weight (a Mettler PM1200 scale) giving a mass fraction accuracy of  $u(w) = 0.00001$ , not taking purity into account. Blends were prepared up to mole fractions of MAPA: 0.75, DAP: 0.81, IPAE: 0.97 and N-TBDEA: 0.36. The lower span for N-TBDEA was due to the high viscosity of the blends.

Titration solutions of  $\text{H}_2\text{SO}_4$  were used to determine the amine concentration in the collected samples from the VLE experiments. Solutions of  $0.1 \text{ mol/dm}^3$  ( $\sim 0.976 \text{ wt\%}$ )  $\text{H}_2\text{SO}_4$  were used for titration of amine samples with high amine content and solutions of  $0.01 \text{ mol/dm}^3$  ( $\sim 0.098 \text{ wt\%}$ )  $\text{H}_2\text{SO}_4$  were used as titrant of low concentration samples.

### 3.2. Density measurements

Pure amine densities were measured at different temperatures up to 363 K. An Anton Paar DMA 4500 densimeter was used for measurements. The densimeter determines the density of a liquid in a U-tube directly from the measured resonance frequency. The nominal repeatability of the instrument is given as  $u(\rho) = 0.01 \text{ kg}\cdot\text{m}^{-3}$  for density and  $u(T) = 0.01 \text{ K}$  for temperature. We have estimated the actual uncertainty in temperature to be  $u(T) = 0.05 \text{ K}$  and in density (0.5 and 1)  $\text{kg}\cdot\text{m}^{-3}$  as given in Table A1. The detailed procedure can be found in our previous work [17].

### 3.3. Świętoślowski ebulliometer

In 1919 Cottrell [18] and Washburn [19] simultaneously published a method for precise measuring of liquid boiling points and described instruments based on the same principle. This

technique is now used as a rapid and robust method of measuring PT data for pure liquids and PTxy data for binary solutions. Accurate data on vapour-liquid equilibrium are important for accurate design of distillation columns and other chemical processing equipment [20].

The ebulliometric method of measuring vapour liquid equilibrium is like the operation of a distillation column at total reflux, see Fig. 1, where heat is provided by a reboiler to produce vapour. The vapour is condensed at the top of column by a condenser and the condensed liquid flows down the column and re-enters the boiler.

Similarly, the modified Świątosławski ebulliometer [21] used in this work is a closed glassware with heater and no outlet stream. Equilibrium is established between liquid and vapour phase after some time. Samples of both liquid and condensed vapour phase can be withdrawn and analysed for amine content. A detailed description of the ebulliometer is given in our previous works [20,22,23], see also Olson [24].

It is important to mention that the Świątosławski ebulliometer is designed for work with liquids only. All chemicals and solutions that are loaded into it should remain in liquid form during operation. Formation of crystals would not allow proper mixing of the boiling liquid, thus preventing reaching the real equilibrium, and could cause damage of the glassware. Pure DAP, IPAE and MAPA are liquids at ambient conditions, but N-TBDEA is a solid and according to the provider's material safety data sheet, has a melting point at 313 K to 318 K. It was therefore pre-heated to 333 K before charging pure N-TBDEA into the Świątosławski ebulliometer. The empty Świątosławski ebulliometer was also pre-heated to 333 K before pure N-TBDEA was charged to avoid crystallization of pure N-TBDEA. Otherwise the experimental procedures in this work were exactly the same as described by Kim *et al.* [20].

Minor uncertainties are coming from pressure and temperature. The nominal accuracy of the pressure gage was 0.05% of full range, which means  $u(P) = 0.1$  kPa. However, because of uneven boiling, the recorded variation in pressure during the experiments was  $u(P) = 0.25$  kPa. The recorded temperature measurements varied within  $u(T) = 0.1$  K.

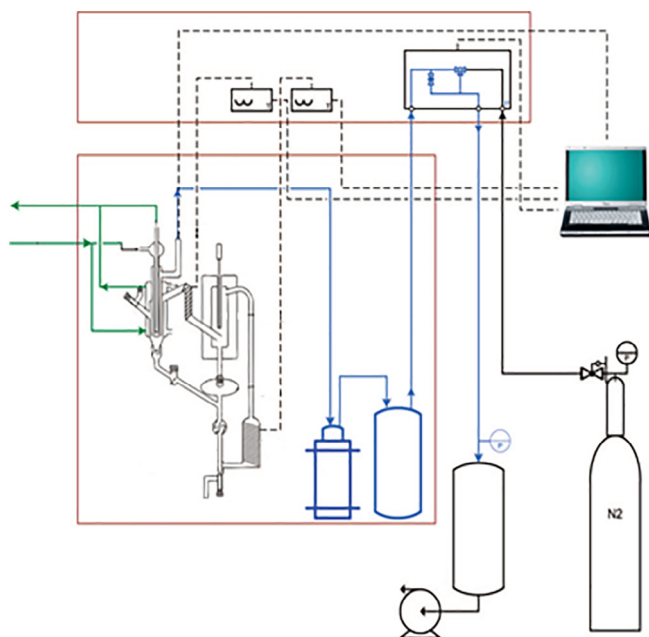


Fig. 1. Simplified scheme of the full ebulliometer installation with gas supply lines and connection to the PC [20].

The major source of uncertainty is the liquid and vapour phase analyses used for the calculation of activity coefficients, see section on sample analyses.

### 3.4. Sample analyses

Titration of the amine solutions was performed using an automatic titration apparatus, a Mettler Toledo G-20, and the LabX software program to register results of the titration. High concentration samples were analysed using  $0.1 \text{ mol/dm}^3$  ( $\sim 0.976 \text{ wt\%}$ )  $\text{H}_2\text{SO}_4$  as titrant and low concentration samples were analysed using  $0.01 \text{ mol/dm}^3$  ( $\sim 0.098 \text{ wt\%}$ )  $\text{H}_2\text{SO}_4$ . The amine titration analyses typically give deviations less than (1 to 3)% between two parallel samples. If larger deviations were observed, more samples were analysed.

The combined composition accuracies vary with amine concentration and system. Based on standard uncertainties in temperature, pressure and amine analyses, the combined uncertainties were estimated to vary significantly. Typically, the uncertainties at low amine concentrations were high both for the liquid and vapour phase. We have noted the appropriate values in Tables A3–A6 in the appendix.

### 3.5. Parameter fitting of thermodynamic model

To calculate the five parameters in the NRTL thermodynamic model, the independent variables, *i.e.*  $x$  and  $T$ , are set in the objective function according to Eq. (5):

$$OF = \sum_{i=1}^N \left( \left| \frac{\mathbb{R}^{Exp} - \mathbb{R}^{Cal}}{\mathbb{R}^{Exp}} \right| \right) \quad (5)$$

where  $\mathbb{R}$  denotes the responses or the dependent variable from the ebulliometric experiment.

Different responses *i.e.* saturation pressure ( $P_i^s$ ), total pressure ( $P_i$ ) and vapour phase composition of amine ( $y_i$ ) were weighed equally in the objective function. An in-house matlab program 'Modfit' for parameter estimation in a general nonlinear multiresponse model was used for the parameter fitting [25].

The absolute average relative deviation (AARD) represents the deviation of the model results from the experimental data as expressed by Eq. (6):

$$AARD_i = \frac{1}{N} \sum_{i=1}^N \left( \left| \frac{\mathbb{R}^{Exp} - \mathbb{R}^{Cal}}{\mathbb{R}^{Exp}} \right| \right) \quad (6)$$

## 4. Results, modelling and discussion

### 4.1. Density measurements

Values of measured density as function of temperature for the pure amines are presented in the appendix in Table A1 and plotted in Fig. 2. The regressed density equations are given in Table 2.

We see that there is a linear relationship between temperature and density for all amines in the range measured. The accuracy of the given correlations is good with an  $R^2$  estimated to be close to unity. Data from Lampreia *et al.* [6] fit very well with our data for IPAE. However, discrepancies exist in the data for MAPA. The difference between data from Wang *et al.* [5] and Liao *et al.* [4] for MAPA is about 1–1.5% as seen in Fig. 2. Based on the supplied purities, we have estimated the uncertainties in our density measurements to be  $u(\rho) = 1 \text{ kg}\cdot\text{m}^{-3}$  for both MAPA and IPAE, see [26]. Thus, the discrepancy between the three measurement sets for MAPA is large. Similar types of densimeters as in this work were used, respectively an SMV 3000 Stabinger and a DMA

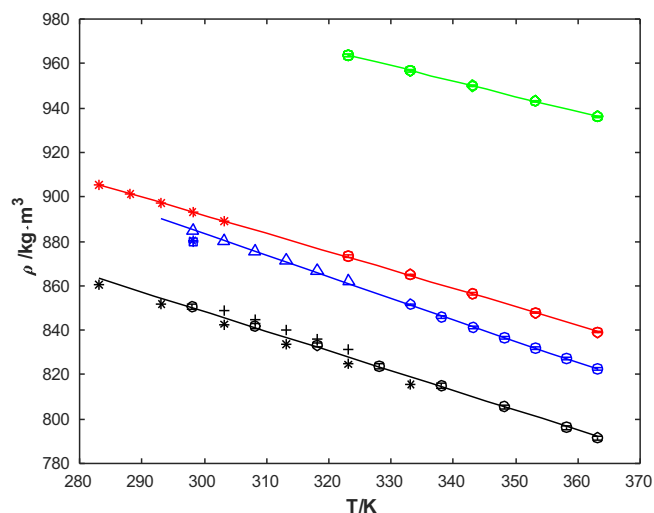


**Fig. 2.** Density of pure amines as a function of temperature (MAPA: ○, This work; ✱, [5]; +, [4]; DAP: ○, This work; △, [7,8]; +, [9]; □, [10]; ✱, [11]; IPAE: ○, This work; ✱, [6]; N-TBDEA: ○, This work; Solid lines, correlations).

**Table 2**  
Density equations for pure amines.

Amine	$\rho/\text{kg} \cdot \text{m}^{-3} = A + B \cdot T/\text{K}$		
	$A \cdot 10^{-3}$	$B$	$R^2$
MAPA	1114.65	-0.8874	0.99061
DAP	1174.13	-0.9688	0.99964
IPAE	1138.28	-0.8220	0.99989
N-TBDEA	1187.24	-0.6915	0.99997

A and B = constants.

$R^2$  = coefficient of determination (R-squared).

5000 M. Our measurements lie between the two literature sources and the temperature dependency shown by the three sets of data is the same. The discrepancies seen may be due to different origins of MAPA with different impurities, since all measurements were done on MAPA as received. In our case the CoA purity given for MAPA was 99.2 wt% and with 0.11 wt% water.

For DAP, our data fit very well with data from Saleh, *et al.* [7,8]. Based on the purity of the supplied DAP, 99.9 wt%, we have estimated the uncertainty in the density measurements to be  $u(\rho) = 0.5 \text{ kg} \cdot \text{m}^{-3}$ . At 298.15 K three more data points exist [9–11]. These three data points are significantly lower than the data from Saleh, *et al.* [7,8].

For N-TBDEA, no prior data were found in the literature. Based on the purity of the supplied N-TBDEA, we have estimated the uncertainty in the density measurements to be  $u(\rho) = 0.5 \text{ kg} \cdot \text{m}^{-3}$ . In this case, we ran two parallels for each temperature. From Table A1, the difference between parallels is seen to be below 0.02%, well below our estimated uncertainty.

#### 4.2. VLE of pure components and binary amine-water mixtures

The pure component vapour pressure results are given in the appendix in Table A2 and the binary VLE data in Tables A3–6.

##### 4.2.1. Pure component data

As mentioned earlier, the ebulliometer measurements were performed as constant pressure measurements, *i.e.* the pressure is set and the temperature to obtain that pressure is measured. For parallel measurements the pressure will therefore typically be the same, as seen in Table A2, and the temperature will vary.

However, the temperature measurements are more accurate than the pressure measurements. Based on this, we have chosen to use the nominal accuracy for temperature,  $u(\rho) = 0.1 \text{ K}$  and attach the total measurement uncertainty to pressure. The standard uncertainty of the pressure measurements in this work is estimated from parallel experiments and varies between amines. The highest uncertainty is found for the lowest temperatures and the lowest uncertainty is for the highest temperatures. The appropriate values are found below Table A2. In all cases the uncertainty is smaller than the circle size in Figs. 3–6.

The data are plotted in Figs. 3–6 and fitted to Antoine equations. The regressed parameters are given in Table 3A together with the accuracy (AARD) for the individual fits. The pure component data were fitted by two alternative methods. In the first method, only the pure component data were considered. In the second method, the pure component data were fitted together with the binary data in a combined fit. Both sets of fitted parameters are given in Table 3A. As mentioned earlier, some of the data for N-TBDEA and DAP were published in anonymized form in Trollebø *et al.* [3]. Unfortunately, the pure component data for N-TBDEA, component B in Table 1 in Trollebø *et al.* [3], are erroneous and should be disregarded.

4.2.1.1. MAPA. As seen in Fig. 3, there are several sources of experimental pure component vapour pressure data for MAPA. Most of the data, Kim *et al.* [20], Hartono *et al.* [23] and Bouzina *et al.* [27], agree very well with each other and also with data obtained in this work. Bouzina *et al.* [27] give the uncertainty of their pressure measurements to be less than 3% of the actual value for the low pressure measurements (<600 Pa) and better than this for higher pressures. This is also smaller than the circle size in Fig. 3. The data of Verevkin and Chernyak [28] in the low temperature range, are low compared to the data from Bouzina *et al.* [27]. The reason may be the use of a dynamic technique, the transpiration method, where gas is blown over a large surface coated with solvent. It may be that vapour-liquid equilibrium is not reached in the exiting gas and thereby the reported values may become too low.

Kim *et al.* [20] provided Antoine parameters and from the blue line in Fig. 3 it is seen that this fitting agrees very well with the

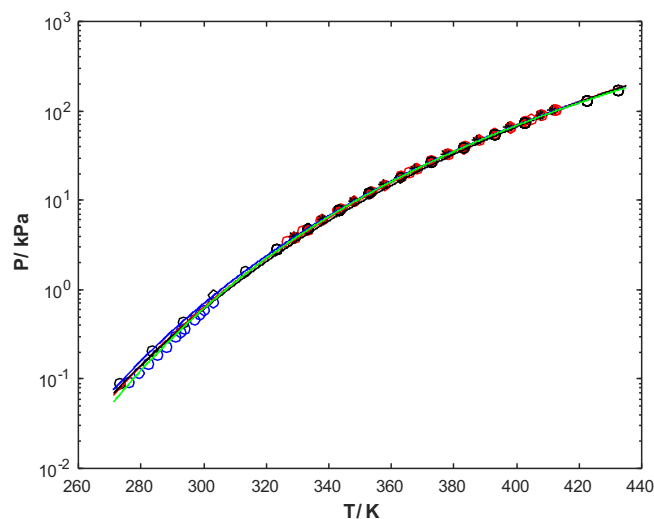


**Fig. 3.** Vapour pressure of pure MAPA. (●, this work; ○, [20]; ✱, [23]; ○, [27]; ○, [28]; Green solid line, fit to only pure component data from all sources; Blue solid line, [20]; Red solid line: fit to combined data from all sources; Black solid line, [29]). (For interpretation of the references to colour in this figure legend, the reader is referred to the web version of this article.)

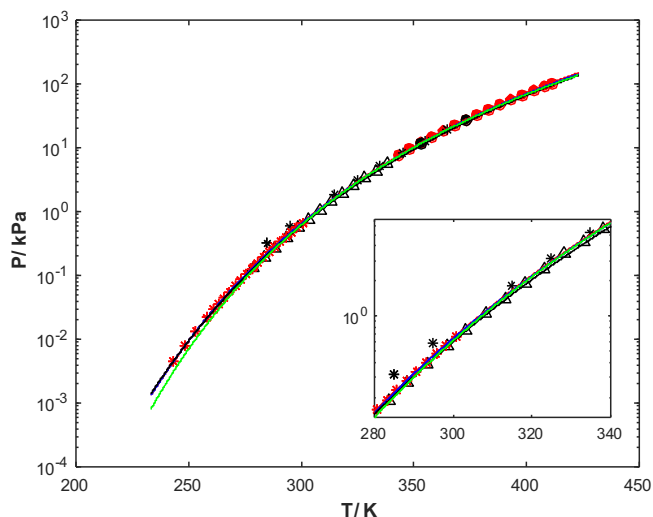


**Fig. 4.** Vapour pressure of pure DAP (●, this work; \*, [30]; △, [31]; ●, [32]; \*, [33]; Blue line: fit to only pure component data from all data, Green line, [32]; Red line: fit to combined data from all data, Black solid line, [29]). (For interpretation of the references to colour in this figure legend, the reader is referred to the web version of this article.)

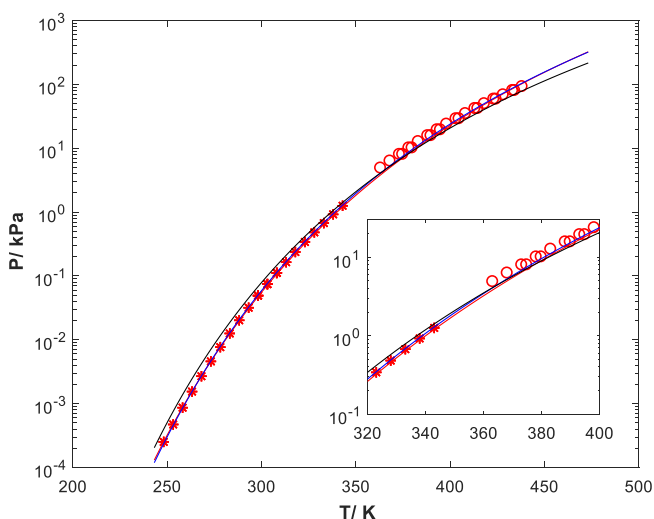


**Fig. 5.** Vapour pressure of pure IPAE (○, this work; \*, [34]; Blue solid line: fit to only pure component data; Red solid line: fit to combined data; Black solid line, [29]). (For interpretation of the references to colour in this figure legend, the reader is referred to the web version of this article.)

data of Bouzina *et al.* [27] at low temperatures and all the higher temperature data. It should be noted that the data by Bouzina *et al.* [27] were not used in this fit. Since we cannot decide for sure what data sets to trust at low temperature, we have used all data in our fits. As seen by the green line in Fig. 3, when fitted to only pure component data, the data by Verevkin and Chernyak [28] pulls the fit down in the low temperature region. This is as expected because of the large number of data points from them. At higher temperatures this fit coincides with the one by Kim *et al.* [20]. When the pure component and binary data were fitted together, shown by the red line in Fig. 3, the pressure curve is pulled upwards in the low temperature region and lies between the fit by Kim *et al.* [20] and our pure component fit. The AARD for the pure component and combined fits are quite similar, respectively 3.1 and 4.5%, as given in Table 3A. The reason for the relatively high AARD values is the discrepancy between the low temperature data. To

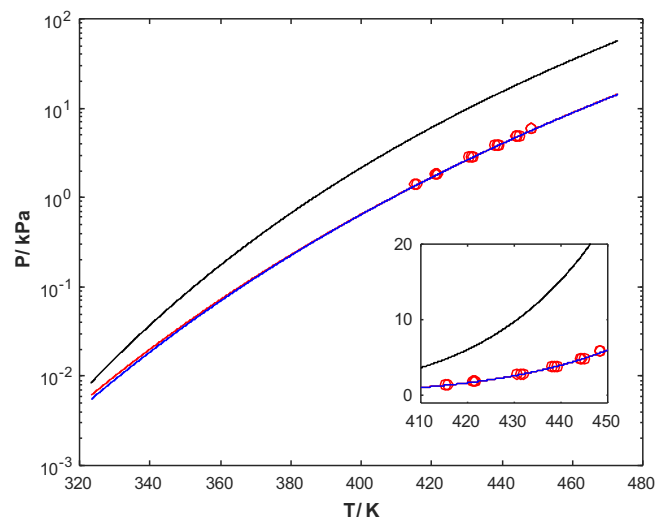


**Fig. 6.** Vapour pressure of pure N-TBDEA. (All points, this work; Blue line: fit to only pure component data; Red line: fit to combined data; Black line, [29]). (For interpretation of the references to colour in this figure legend, the reader is referred to the web version of this article.)

resolve this, more data in this range are needed. It can be noted that by omitting the data by Verevkin and Chernyak [28] in the fitting, the AARD values go down to respectively 1.5% and 2%.

A curve based on the Antoine parameters provided by Yaws *et al.* [29] is also shown in Fig. 3. These parameters give vapour pressures slightly lower than the experimental values. The discrepancy is largest in the middle temperature range.

The water content in the MAPA used in these tests was given as 0.11 wt% which corresponds to approximately a mole fraction of 0.0051. Assuming an ideal solution, the contribution of water to the total pressure measured was found to be <2% for all cases. The pressures given in Table A2 are the measured total pressures and not corrected for water pressure.

**4.2.1.2. DAP.** For DAP, some pure component vapour pressure data exist. Ahmed, *et al.* [30] provide data for the low and middle temperature region, data from Pozdeev and Verevkin [31] cover the low temperature region, whereas this work provides data for the middle to higher temperatures. In addition there are two data points from Pividal and Sandler [32] in the middle temperature region. Very recently Fulem, *et al.* [33] reported data for the low and the middle temperature region. All data are shown in Fig. 4.

Most of the data are in good agreement. The data from Ahmed *et al.* [30] seem to be slightly high, but also in reasonable agreement with the rest. Data from Pozdeev and Verevkin [31] fill the gap between the low temperature data of Fulem, *et al.* [33] and our data. Based on their two data points, which fit well with our data, Pividal and Sandler [32] postulated an Antoine equation, the green line in Fig. 4, which agrees with the data of Pozdeev and Verevkin [31], but deviates from the data of Fulem, *et al.* [33] in the low temperature range. The Antoine equation given by Yaws *et al.* [29] agrees well with the data.

The pure component and combined fits, both based on data from this work and all data from the literature, as shown by the red and blue lines respectively in Fig. 4, give very similar results. The pure component and combined fit AARDs are 2.1 and 2.7% respectively as shown in Table 3A.

**4.2.1.3. IPAE.** For IPAE, Soares *et al.* [34] reported data from 250 K to 350 K covering the low temperature region. The data provided in this work comprises two individual measurement series performed



**Table 3A**  
Parameters in the Antoine equation for pure MAPA, DAP, IPAE and N-TBDEA.

Amine	A	$u(A)$	B	$u(B)$	C	$u(C)$	AARD/%
MAPA	6.3	0.2	-1431	80	-80	7	4.5
	5.8	0.1	-1184	38	-104	4	3.1*
DAP	6.8	340	-1659.4	34,000	-61.21	3400	2.7
	6.7	340	-1640.2	34,000	-61.99	3400	2.1*
IPAE	8.2	8	-2464.8	7000	-39.0	700	5.9
	7.9	245	-2267.9	24,000	-51.02	2400	4.4*
N-TBDEA	9.0	4	-3916	3800	25.61	220	1.6
	8.6	4	-3499	3200	0.61	200	1.6*

A, B and C are constants.

$u(A)$ ,  $u(B)$  and  $u(C)$  are standard deviation of the parameters.

In Table 3A the fitted parameters are given both for the combined fit with binary data and for the direct fit to only pure component data (marked \*).

over a period of several months and covers the high temperature region. The reproducibility between the three sets is seen in Fig. 5 to be acceptable, but one of the sets give slightly lower values than the others. This set, however, agrees best with the data reported by Soares *et al.* [34]. Both a combined fit with binary data and one only based on the pure component data were performed, using all data in Fig. 5. Fig. 5 shows that both methods give similar results and the AARD's given in Table 3A were 4.4% for only pure component data and 5.9% for the combined fit.

Predictions based on Antoine parameters from Yaw's *et al.* [29], given by the black line in Fig. 5, are shown to over-predict the vapour pressure in the low temperature region and under-predict in the high temperature region compared to the experimental data.

**4.2.1.4. N-TBDEA.** No pure component vapour pressure data were found for N-TBDEA in the literature, disregarding the erroneous data in Trollebø *et al.* [3]. The data sets provided in this work consist of 16 data points, all in the high temperature range. The reason for this is that the pure component vapour pressures were very low such that the accuracy became unsatisfactory at lower temperatures. The data are based on three data sets obtained at different times. The purity given by the provider (Sigma-Aldrich) was the same for all N-TBDEA batches received. However, two of the batches were solid, whereas the third was in liquid form. This is in line with the information provided by the Sigma-Aldrich data sheet. All vapour pressure data obtained, as given in Fig. 6 and Table A2, are for temperatures above the N-TBDEA melting point, *i.e.* for the liquid state. The data in Fig. 6 show excellent reproducibility and that no difference in vapour pressure exists between the batches. The pure vapour pressure data were used in the NRTL model for binary data in a combined fit. Since the binary data only go up to 373 K, small uncertainties in the pure component model could result in discrepancies in the binary model. Thus, in this case, fitting the binary and pure component data together was a necessity. We see in Fig. 6 that a small difference between the pure component and combined fits exists. However, the differences seen in the lower temperature range did not result in any difference in AARD between the pure component and combined fits, both being 1.6%, as seen in Table 3A. This is because the curves overlap in the range where experimental pure component data exist as shown in the magnified part of Fig. 6.

Predictions based on Antoine parameters from Yaw *et al.* [29], given by the black line in Fig. 6, are shown to be much too high compared to the experimental data in the experimental temperature range.

Table 3A shows that the standard deviations on the parameters are reasonable only for MAPA. For DAP, IPAE and N-TBDEA, the standard deviations in the B and C parameters are of the same size as, or larger than the parameter values. This indicates that the objective function probably has a flat optimum and that several possible parameter combinations exist, giving approximately the same goodness of fit.

In Table 3B is shown a comparison between pure component pressure data and predictions from the combined fit model, based on both pure component and binary data, for the various data sets.

For MAPA we see that the AARDs for the data set of Verevkin and Chernyak [28] is higher than for the other sets, and the data are on the low side as commented earlier. For DAP, the data set from Ahmed *et al.* [30] give higher AARD than the other data and over-predict the vapour pressures slightly as mentioned earlier. For IPAE, a small discrepancy between our data and the data of Soares *et al.* [34] seem to exist. However, the data sets are obtained in different temperature regions and data for the middle region should be obtained.

#### 4.2.2. Binary systems

The experimental data for the MAPA(1)/H<sub>2</sub>O(2), DAP(1)/H<sub>2</sub>O(2), IPAE(1)/H<sub>2</sub>O(2) and N-TBDEA(1)/H<sub>2</sub>O(2) systems are given in the appendix, Tables A3–6. Some of the data were previously published in anonymized form in Trollebø *et al.* [3], but with several mistakes. In Table 3 in Trollebø *et al.* [3], all pressures are in mbar, not kPa as said in the table heading. In Table 4 in Trollebø *et al.* [3], for 60 and 100 °C the temperature columns actually give the pressures in kPa and the pressure columns give pressures in mbar. The corrected data are found in Tables A3–A6.

The plots of data plus the NRTL model representations are given below. Regressed NRTL model parameters were calculated using both the combined pure component and binary experimental VLE data and separate pure component and binary fits and are given in Table 4A and 4B. It should be noted that all amines are assumed to behave as non-dissociated species because of their high pK<sub>a</sub> values. A thorough explanation can be found in our previous work [22]. All the fits were made based on mole fractions. The largest uncertainties in the data are the liquid and gas phase analyses, in particular for low mole fractions. The estimated standard uncertainties vary and are given below Tables A3–A6.

**4.2.2.1. MAPA.** In Fig. 7A shows PT<sub>xy</sub> data for the MAPA(1)/H<sub>2</sub>O(2) system based on data from Kim *et al.* [20] covering the temperature range from 313 K to 373 K, and from the present work at 333 K and 353 K. The data sets are seen to agree well in the range of low MAPA contents, below a mole fraction of about 0.25. However, above this level, the data from Kim *et al.* [20] show higher pressures than the data from the present work. Data from Bouzina *et al.* [27] are also given and are shown to agree well with data from the present work. The model fit based on the combined pure component and binary data from this work, Kim *et al.* [20] and Bouzina *et al.* [27], as shown in Fig. 7, agree well with the binary data with an AARD for pressure of 3.9% as shown in Table 4A.

In the work of Bouzina *et al.* [27] only PT<sub>x</sub> data are given. A comparison between model predicted and experimental equilibrium pressures as function of composition and temperature is given in Fig. 7B. We see that the model is able to represent the data very well up to a MAPA weight fraction of about 0.75. This is high

**Table 3B**

Absolute Average Relative Deviations (AARD) between the combined fit for the Antoine models and the various data sources.

MAPA		DAP		IPAE	
AARD/%	Reference(s)	AARD/%	Reference(s)	AARD/%	Reference(s)
1.3	This work	2.7	This work	10.8	This work
3.7	[23]	11.9	[30]	3.0	[34]
3.1	[20]	2.8	[32]		
3.8	[27]	5.6	[31]		
13.3	[28]	0.9	[33]		
4.5	[20,23,27,28] and this work	2.7	[30,31,32,33] and this work	5.9	[34] and this work

**Table 4A**

Fitted parameters in the Non-Random Two-Liquid (NRTL) model (combined fitting) with their Absolute Average Relative deviation (AARD) values.

Binary system	NRTL parameter										AARD/%	
	$A_{12}$	$u(A_{12})$	$B_{12}$	$u(B_{12})$	$A_{21}$	$u(A_{21})$	$B_{21}$	$u(B_{21})$	$\alpha$	$u(\alpha)$	P	$y_1$
MAPA(1)/H <sub>2</sub> O(2)	-4194.5	172	8.5	1	8026.1	392	-27.9	6	0.93	0.05	3.9	10.4
DAP(1)/H <sub>2</sub> O(2)	-5364.96	3041	7.81	6	1794.68	3040	-9.17	31	0.50	0.31	1.7	11.9
IPAE(1)/H <sub>2</sub> O(2)	-1262.9	1383	2.88	8	2835.2	6911	47.0	70	0.58	0.69	2.9	6.9
N-TBDEA(1)/H <sub>2</sub> O(2)	-978.1	1237	31.8	18	3579.1	1222	63.3	17	0.66	0.03	1.1	-

A, B and  $\alpha$  = binary interaction parameters and non-randomness. $u(A)$ ,  $u(B)$ , and  $u(\alpha)$  = standard deviation of the parameters.

P and y = Total Pressure and vapour-phase composition.

1, 2 = components.

**Table 4B**

Fitted parameters in the Non-Random Two-Liquid (NRTL) model with their Absolute Average Relative deviation (AARD) values (individual pure component and binary fits).

Binary system	NRTL parameter										AARD/%	
	$A_{12}$	$u(A_{12})$	$B_{12}$	$u(B_{12})$	$A_{21}$	$u(A_{21})$	$B_{21}$	$u(B_{21})$	$\alpha$	$u(\alpha)$	P	$y_1$
MAPA(1)/H <sub>2</sub> O(2)	-4217.5	160	8.0	1	7906.6	400	-24.7	6	0.92	0.05	4.2	10.7
DAP(1)/H <sub>2</sub> O(2)	-5324.2	3000	7.35	6	1783.12	3000	-7.17	30	0.51	0.3	1.8	12.1
IPAE(1)/H <sub>2</sub> O(2)	-1290.6	1000	1.01	6	2507.8	5200	52.5	53	0.57	0.5	3.3	10.1
N-TBDEA(1)/H <sub>2</sub> O(2)	-978.1	1250	31.8	18	3579	1250	63.3	17	0.66	0.02	1.1	-

A, B and  $\alpha$  = binary interaction parameters and non-randomness. $u(A)$ ,  $u(B)$ , and  $u(\alpha)$  = standard deviation of the parameters.

P and y = Total Pressure and vapour-phase composition.

1, 2 = components.

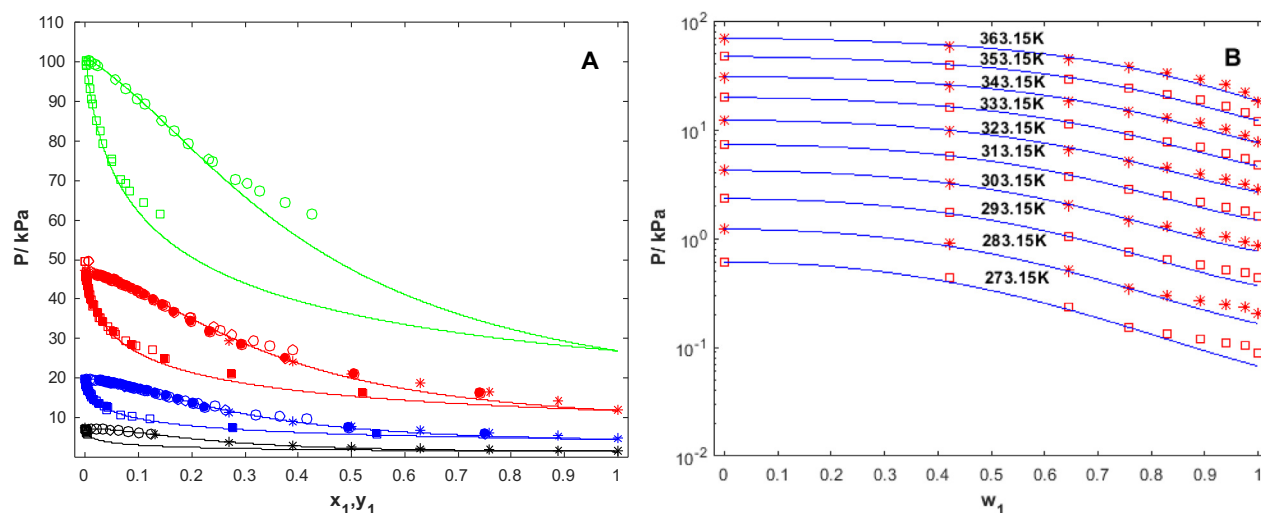


**Fig. 7.** Calculated and experimental PTxy data of the MAPA(1)/H<sub>2</sub>O(2) system at different temperatures. A). Filled Points, this work; Unfilled points, [20]; Stars, (Bouzina *et al.* 2016). Solid lines NRTL model based on data from this work, Kim *et al.* [20] and Bouzina *et al.* [27]; Black, 313 K; Blue, 333 K; Red, 353 K; Green, 373 K). B). Points, [27]; Solid lines NRTL model. (For interpretation of the references to colour in this figure legend, the reader is referred to the web version of this article.)

enough for all practical interest. Above this value, discrepancies exist and become larger for lower temperatures.

In Fig. 8, calculated activity coefficients are given for the present data sets and for data from Kim *et al.* [20]. As indicated by the pres-

ures reported by Kim *et al.* [20], shown in Fig. 7A, the water activity coefficients based on that work, above a MAPA mole fraction of 0.25, deviate both from the model and from activity coefficients calculated from data in the present study. Actually, deviations from

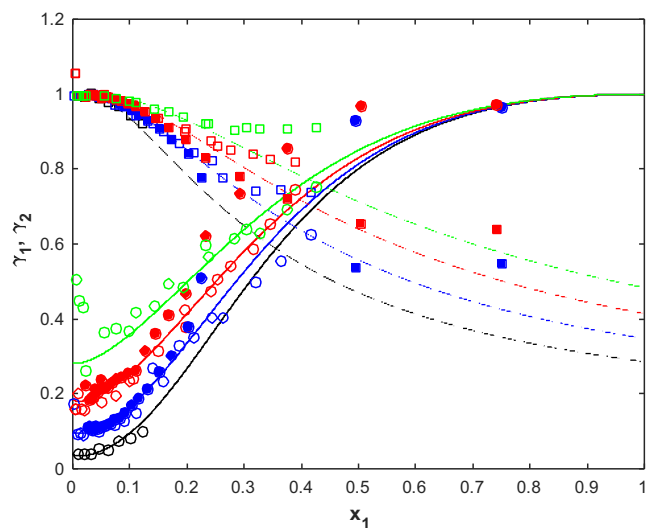


**Fig. 8.** Calculated and experimental activity coefficients for MAPA(1)/H<sub>2</sub>O(2). Experimental data; solid points, this work; open points, [20]. NRTL model: Solid lines MAPA, dashed lines water. Black 313 K, blue 333 K; red 353 K, green 373 K. (For interpretation of the references to colour in this figure legend, the reader is referred to the web version of this article.)

their own developed model were already reported in Kim *et al.* [20]. For lower MAPA concentrations, both data sets and the model agree very well with a MAPA vapour phase composition AARD of 10.4%, see Table 4A.

In Table 4B are given results for the separate fitting of pure component and binary data. For MAPA we see that the parameters change slightly, but the AARDs for both pressure and MAPA activity coefficient remain almost the same. This is also shown in Figs. S6 and S7 in the supplementary information, which are nearly identical to Figs. 7 and 8.

With PTxy data it is possible to check the thermodynamic consistency according to the Gibbs-Duhem equation, see Kim *et al.* [20], Van Ness and Iserman [35] and Prausnitz *et al.* [36]. The NRTL model is inherently thermodynamic consistent, so parity plots between experimental data and model will give a good indication of the consistency of the data. Fig. S1 in the supplementary

information shows parity plots for the model and the present data, indicating good thermodynamic consistency for MAPA. Bouzina *et al.* [27] provided only PTx data, but calculated y-values. The thermodynamic consistency of these data is given in Fig. S2 in the supplementary information and indicates that their calculated vapour compositions should be used with care.

4.2.2.2. DAP. Fig. 9A shows PTxy data for the DAP(1)/H<sub>2</sub>O(2) system based on data from the present work at 343 K, 353 K and 373 K. PTx data from Ahmed *et al.* [30] are also given and are shown to agree well with data from the present work. The model fit based on the combined pure component and binary data from this work and [30], as shown in Fig. 9A, agree well with the data with an AARD for pressure of 4.2% as shown in Table 4A.

Fig. 9B shows a comparison between the developed NRTL model and the full data set from Ahmed *et al.* [30]. The agreement is excellent up to an amine weight fraction of about 0.6, covering the most interesting industrial range. Above this value, the discrepancies between model and experimental data increase with amine content and with decreasing temperature. At the lowest temperatures, (293 K and 303 K), the experimental data show unexpected increases in vapour pressure around an amine weight fraction of 0.9. The NRTL model seems to indicate a very weak azeotrope around 0.9 in amine mole fraction. No experimental data exist to validate this. The AARD for pressure is 1.7% as given in Table 4A.

Fig. 10 compares experimental and NRTL-model based activity coefficients for the DAP(1)/H<sub>2</sub>O(2) system. Water activity coefficients are predicted well over the whole experimental concentration range, whereas the activity coefficients for DAP are under-predicted above amine mole fractions of about 0.3. The AARD for the fit of DAP vapour phase composition is 11.9% as seen in Table 4A.

Results from the model based on a separate fit of pure component and binary data are shown in Figs. S8 and S9 in the supplementary information and these are almost identical to Figs. 9 and 10. Table 4B shows the AARDs for P and y this case, respectively 1.8 and 12.1%, only marginally higher than for the combined fit. Both the binary system fits and pure component fits are quite close, with AARDs of 2.1 and 2.7% respectively, the choice of fitting method seems not important in this case. Tables 4A and 4B also give standard deviations on the parameters. We see that for DAP, the standard deviations are larger, and for some parameters much

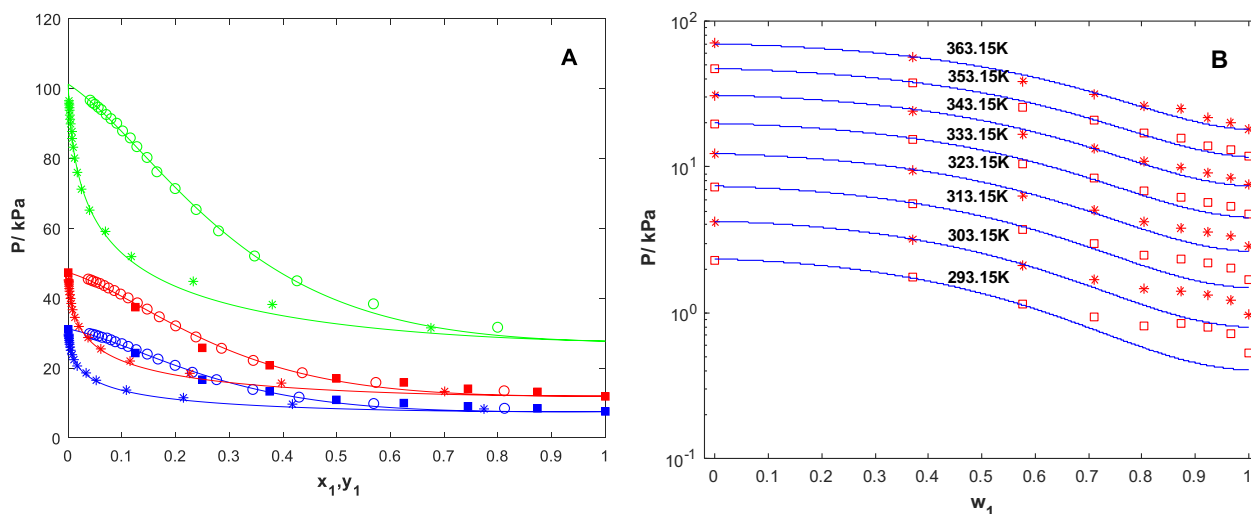


**Fig. 9.** Calculated and experimental PTx data of the DAP(1)/H<sub>2</sub>O(2) system at different temperatures. A) Experimental data; circles and stars, this work, filled squares, [30]. Solid lines: NRTL model based on data from this work and [30]. Blue 343 K; red 353 K, green 373 K. B) Points, [30]; Solid lines, NRTL model. (For interpretation of the references to colour in this figure legend, the reader is referred to the web version of this article.)



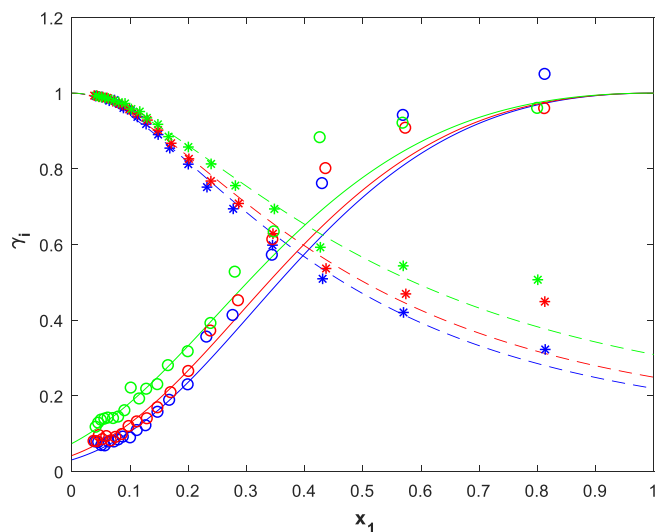


**Fig. 10.** Calculated and experimental activity coefficients for DAP(1)/H<sub>2</sub>O(2). Experimental data; all points this work. NRTL model: Solid lines DAP, dashed lines water. Blue, 343 K; red, 353 K; Green, 373 K. (For interpretation of the references to colour in this figure legend, the reader is referred to the web version of this article.)

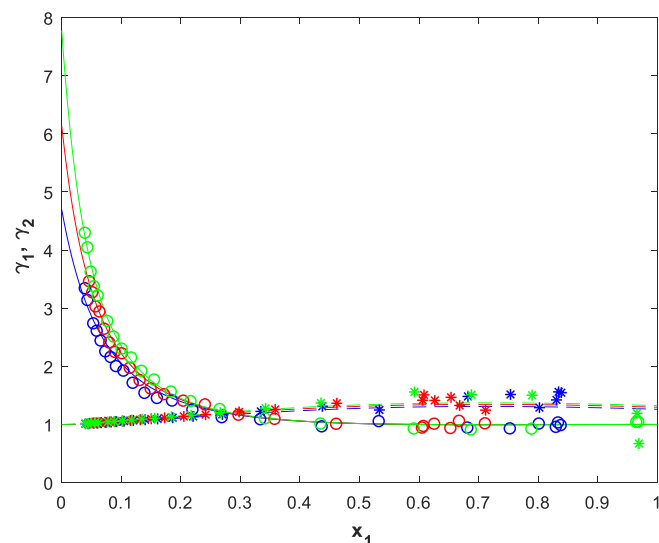


**Fig. 12.** Calculated and experimental activity coefficients for IPAE(1)/H<sub>2</sub>O(2). Experimental data; all points this work. NRTL model: Solid lines IPAE, dashed lines water. Blue, 333 K; Red, 353 K; Green, 373 K. (For interpretation of the references to colour in this figure legend, the reader is referred to the web version of this article.)

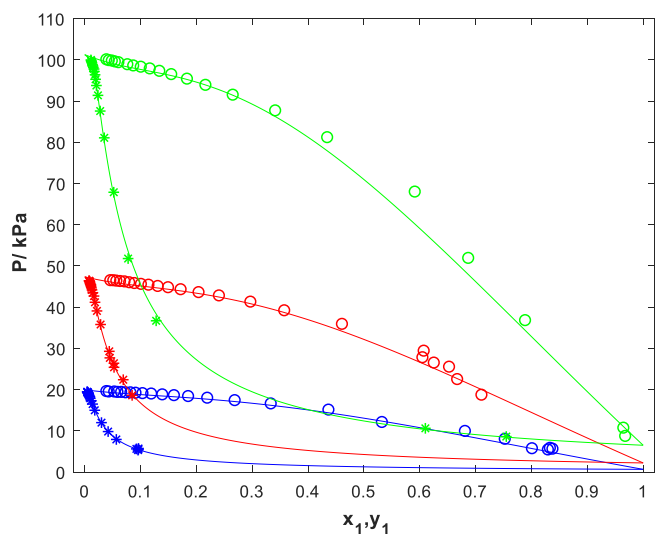


**Fig. 11.** Calculated and experimental PTxy data of the IPAE(1)/H<sub>2</sub>O(1) system at different temperatures. Experimental data; all points this work. NRTL model: Solid lines. Blue, 333 K; Red, 353 K; Green, 373 K. (For interpretation of the references to colour in this figure legend, the reader is referred to the web version of this article.)

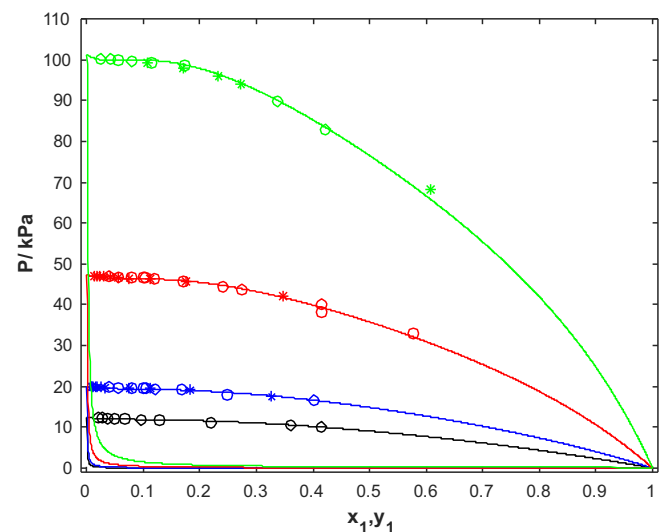


**Fig. 13.** Calculated and experimental PTx data of the N-TBDEA(1)/H<sub>2</sub>O(2) system at different temperatures. Experimental data (circles, [3]; stars, this work; all points this work. NRTL model: Solid lines. Black, 323 K; Blue, 333 K; Red, 353 K; Green, 373 K. (For interpretation of the references to colour in this figure legend, the reader is referred to the web version of this article.)

larger, than the parameters themselves. This indicates a flat objective function optimum for the binary fit and that several possible parameter combinations may give approximately the same goodness of fit.

Fig. S3 in the supporting information shows that the thermodynamic consistency of the data is good.

**4.2.2.3. IPAE.** Fig. 11 shows PTxy data for the IPAE(1)/H<sub>2</sub>O(2) system based on data from the present work at 333 K, 353 K and 373 K. No data for this system were found in the literature. The model fit based on the combined pure component and binary data, as shown in Fig. 11, agree well with the data with an AARD for pressure of 2.9% as shown in Table 4A. The largest deviations between model and experimental data are found for 373 K and at the intermediate amine concentrations.

Fig. 12 compares experimental and NRTL-model based activity coefficients for the IPAE(1)/H<sub>2</sub>O(2) system. What characterizes this system is the apparently very low temperature sensitivity of the activity coefficients. The scatter in the data, notably in the higher amine concentration range, is larger than the model predicted temperature sensitivity. It should be noted that the pure component fit will influence the activity coefficients calculated from the experimental data, and thereby the binary model temperature sensitivity. The AARD for the fit of IPAE vapour phase composition is 6.9% as seen in Table 4A. As for DAP, the standard deviations on the parameters are of the same size or larger than the parameters. Fig. S4 in the supporting information shows that the thermodynamic consistency of the data is reasonable, apart from at the higher amine concentrations where the data scatter is the highest.

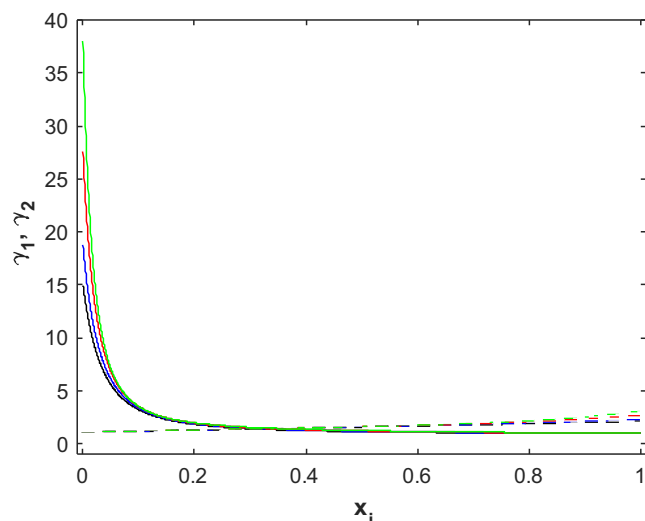


**Fig. 14.** Calculated activity coefficients for N-TBDEA(1)/H<sub>2</sub>O(2). NRTL model: Solid lines N-TBDEA, dashed lines water. Black, 323 K; Blue, 333 K; Red, 353 K; Green, 373 K. (For interpretation of the references to colour in this figure legend, the reader is referred to the web version of this article.)

The reason for the larger scatter in the data for the IPAE(1)/H<sub>2</sub>O(2) system compared to MAPA and DAP, is believed to be due to the significantly lower volatility of IPAE and thereby higher uncertainty in the gas phase analyses. In Fig. 11, we also see that the gas phase curves are close to flat in the higher concentration range. This makes the activity coefficients very sensitive to small errors in the gas phase composition analysis.

Fitting the pure component and binary data separately was also done. The results are given in Table 4B and shown graphically in

Figs. S10 and S11 in the supporting information. We see that the AARDs for pressure and vapour phase composition rise to 3.3 and 10.1% respectively. Also, the standard deviations on the parameters become higher than the parameters themselves. Clearly, a combined fit gives a better result in this case. This was not the conclusion for DAP and the reason for this difference is believed to be the amine volatility. The fit of the binary data will depend on the pure component data and the fit to these data. When the amine volatility is low, the sensitivity to errors in the pure component data is high, whereas when the volatility is high, this reduces the sensitivity to errors in the pure component data. In addition, the pure component data for IPAE only extended down to 363 K. In order to validate the model further, more pure component data are needed, particularly for temperatures below 363 K.

**4.2.2.4. N-TBDEA.** N-TBDEA is the amine, among the four studied in this work, that has the lowest volatility. In the ebulliometer, the gas phase concentrations became so low that they were below the quantification limit using the titration methods in this work. Only PTx data are thus available, as shown in Fig. 13. The model fit in Fig. 13 is for the combined data and the AARD on pressure is 1% as shown in Table 4A.

Fig. 14 shows the calculated activity coefficients. We see that the predicted amine activity coefficients become very large at low concentrations. This should be taken as an indication only, and vapour composition data are needed to validate the model. The situation is similar for the predicted water activity coefficients at low water concentrations. They are seen to increase to values 2 to 3.

Fitting the parameters to pure component and binary data separately was also done in this case. The fits are shown in Figs. S12 and S13 in supporting information and the AARD is given in Table 4B. The AARD did not change and no visible effect is seen

**Table 4C**

Absolute Average Relative Deviations (AARD) between the combined fit for the Non-Random Two-Liquid (NRTL) model and the various data sources.

MAPA			DAP		
AARD/%		Reference(s)	AARD/%		Reference(s)
P	y <sub>1</sub>		P	y <sub>1</sub>	
1.1	7.6	This work	1.7	12.2	This work
2.1	12.5	[20]	23.8	–	[30]
6.4	–	[27]			
3.9	10.4	[20, 27] and this work	1.8	12.2	[30] and this work

P and y = Total Pressure and vapour-phase composition.

1 = Amine.

**Table A1**

Density  $\rho$  data for pure amines at temperature T and ambient pressure P\*.

DAP		IPAE		MAPA		N-TBDEA	
T/K	$\rho/\text{kgm}^{-3}$	T/K	$\rho/\text{kgm}^{-3}$	T/K	$\rho/\text{kgm}^{-3}$	T/K	$\rho/\text{kgm}^{-3}$
333.15	851.50	323.13	873.16	298.12	850.66	323.13	963.63
338.15	845.75	333.12	864.93	308.12	841.79	323.13	963.79
343.15	841.13	343.12	856.49	318.12	833.34	333.12	956.91
348.15	836.52	353.17	847.91	328.12	823.77	333.12	956.93
353.15	831.87	363.12	839.14	338.12	815.03	343.12	949.99
358.15	827.23	–	–	348.12	805.53	343.12	950.07
363.15	822.69	–	–	358.12	796.19	353.12	943.07
–	–	–	–	363.12	791.51	353.12	943.05
–	–	–	–	–	–	363.12	936.07
–	–	–	–	–	–	363.12	936.07
Standard uncertainties							
$u(T) = 0.05 \text{ K}$		$u(T) = 0.05 \text{ K}$		$u(T) = 0.05 \text{ K}$		$u(T) = 0.05 \text{ K}$	
$u(\rho) = 0.5 \text{ kgm}^{-3}$		$u(\rho) = 1 \text{ kgm}^{-3}$		$u(\rho) = 1 \text{ kgm}^{-3}$		$u(\rho) = 0.5 \text{ kgm}^{-3}$	

\* Atmospheric pressure (101 ± 3)kPa.

**Table A2**

Boiling point values\* for pure components (N-*tert*-Butyldiethanolamine/N-TBDEA, 2-(Isopropylamino)ethanol/IPAE, 1,3-diaminopropane/DAP and N-Methyl-1,3-diaminopropane/MAPA) at temperature T and pressure P.

N-TBDEA**			IPAE			DAP			MAPA		
T/K	P/kPa	u(P)/kPa	T/K	P/kPa	u(P)/kPa	T/K	P/kPa	u(P)/kPa	T/K	P/kPa	u(P)/kPa
Exp. 1			363.2	4.9	0.4	343.2	7.5	0.3	329.2	3.8	0.25
415.9	1.4	0.25	368.2	6.3	0.5	348.2	9.5	0.3	333.3	4.7	0.3
421.8	1.8	0.25	373.2	8.0	0.6	353.3	11.9	0.4	338.2	6.0	0.3
432.1	2.8	0.25	374.9	8.0	0.6	358.1	14.7	0.4	343.1	7.6	0.4
439.4	3.8	0.25	378.2	10.1	0.7	363.2	18.2	0.5	348.2	9.6	0.5
445.1	4.8	0.25	379.9	10.1	0.7	368.2	22.3	0.6	353.2	12.0	0.6
Exp. 2			383.2	12.7	0.7	373.2	27.1	0.7	358.1	14.8	0.7
415.9	1.4	0.25	388.2	15.7	0.8	378.2	32.7	0.9	363.3	18.3	0.9
421.8	1.8	0.25	389.9	15.7	0.8	383.2	39.3	1.0	368.2	22.3	1.0
432.1	2.8	0.25	393.2	19.4	0.9	388.2	47.0	1.1	373.2	27.1	1.1
439.4	3.8	0.25	394.9	19.4	0.9	393.2	55.9	1.2	378.2	32.6	1.2
445.1	4.8	0.25	398.2	23.8	1.1	398.3	66.0	1.4	383.2	37.8	1.3
Exp. 3			403.2	28.9	1.3	403.2	77.6	1.6	388.2	46.5	1.4
415.5	1.4	0.25	404.8	28.9	1.3	408.2	90.8	1.8	393.2	55.2	1.5
421.2	1.8	0.25	408.2	34.8	1.5	411.4	100.0	2.0	398.2	65.1	1.6
431.6	2.8	0.25	413.2	41.8	1.8	–	–	–	403.2	76.3	1.7
438.8	3.8	0.25	414.7	41.8	1.8	–	–	–	408.2	89.2	1.8
444.5	4.8	0.25	418.2	49.7	2.0	–	–	–	412.2	100.7	2.0
448.4	5.8	0.25	423.2	58.6	2.2	–	–	–	–	–	–
–	–	–	424.4	58.5	2.2	–	–	–	–	–	–
–	–	–	428.2	68.5	2.5	–	–	–	–	–	–
–	–	–	433.2	80.0	3.0	–	–	–	–	–	–
–	–	–	434.3	80.0	3.0	–	–	–	–	–	–
–	–	–	438.2	92.1	3.5	–	–	–	–	–	–
u(T) = 0.1 K			u(T) = 0.1 K			u(T) = 0.1 K			u(T) = 0.1 K		

\* Uncertainties, u, are given as standard uncertainties. Data in italics are previously published in anonymized form in Trollebø *et al.* [3].

\*\* N-TBDEA in all experiments was above the melting point, *i.e.* in liquid state.

**Table A3**

Experimental (vapour + liquid) data for temperature T, pressure P, liquid-phase mole fraction  $x_1$ , and gas-phase mole fraction  $y_1$ , for N-Methyl-1,3-diaminopropane/MAPA(1) + H<sub>2</sub>O(2)\*.

T/K	P/kPa	$x_1$	u( $x_1$ )	$y_1$	u( $y_1$ )	T/K	P/kPa	$x_1$	u( $x_1$ )	$y_1$	u( $y_1$ )
333.2	6.0	0.7505	0.008	0.5466	0.0060	353.2	16.3	0.7423	0.008	0.5215	0.0060
333.1	7.5	0.4951	0.006	0.2779	0.0050	353.2	21.1	0.5055	0.006	0.2736	0.0050
333.2	12.5	0.2247	0.005	0.0415	0.0020	353.2	25.1	0.3763	0.006	0.1511	0.0040
333.3	13.7	0.2020	0.005	0.0253	0.0015	353.2	28.6	0.2934	0.005	0.0887	0.0030
333.2	14.7	0.1738	0.004	0.0162	0.0013	353.2	31.8	0.2335	0.005	0.0537	0.0020
333.2	15.5	0.1514	0.004	0.0114	0.0009	353.2	34.4	0.1988	0.004	0.0319	0.0018
333.2	16.2	0.1319	0.004	0.0078	0.0007	353.2	36.7	0.1675	0.004	0.0220	0.0014
333.3	16.8	0.1162	0.004	0.0059	0.0005	353.2	38.5	0.1457	0.004	0.0161	0.0013
333.2	17.2	0.1036	0.004	0.0046	0.0005	353.2	39.9	0.1276	0.004	0.0118	0.0009
333.2	17.6	0.0921	0.004	0.0035	0.0004	353.2	41.0	0.1115	0.004	0.0084	0.0007
333.2	17.9	0.0825	0.004	0.0028	0.0004	353.2	42.0	0.0976	0.004	0.0070	0.0006
333.2	18.2	0.0741	0.003	0.0024	0.0003	353.2	42.8	0.0861	0.004	0.0058	0.0005
333.2	18.4	0.0671	0.003	0.0020	0.0003	353.2	43.3	0.0768	0.003	0.0050	0.0005
333.2	18.6	0.0603	0.003	0.0017	0.0003	353.2	43.8	0.0684	0.003	0.0042	0.0004
333.2	18.7	0.0544	0.003	0.0015	0.0003	353.2	44.3	0.0613	0.003	0.0035	0.0004
333.2	18.9	0.0489	0.003	0.0013	0.0002	353.2	44.7	0.0494	0.003	0.0031	0.0004
333.2	19.0	0.0440	0.003	0.0011	0.0002	353.2	44.9	0.0550	0.003	0.0031	0.0004
333.2	19.1	0.0403	0.003	0.0011	0.0002	353.2	45.2	0.0451	0.003	0.0024	0.0003
333.3	19.2	0.0366	0.003	0.0009	0.0002	353.2	45.4	0.0400	0.003	0.0022	0.0003
333.2	19.3	0.0334	0.003	0.0008	0.0002	353.2	45.6	0.0365	0.003	0.0018	0.0003
333.2	19.3	0.0304	0.003	0.0008	0.0002	353.2	45.8	0.0331	0.003	0.0016	0.0003
333.2	19.4	0.0273	0.002	0.0007	0.0002	353.2	45.9	0.0299	0.002	0.0014	0.0003
–	–	–	–	–	–	353.2	46.0	0.0229	0.002	0.0013	0.0003

\* Standard uncertainties u are u(T) = 0.1 K; u(P) = 0.25 kPa.

in Figs. S12 and S13. The main reason for this is the large difference in temperature range between the pure component (413 K to 453 K) and binary (313 K to 373 K) data. We see in Fig. 6 that using a combined fit only has a small impact on the pure component predictions, even at lower temperatures.

In Table 4C is shown a comparison between binary pressure and vapour mole fraction data and predictions from the combined fit model for the various data sets.

For total pressure we see that the data from Bouzina *et al.* [27] and Ahmed *et al.* [30] give higher AARDs than the other data. The

main reason for this is the deviations in pressure seen in Figs. 7B and 9B at high amine mole fractions.

4.2.2.5. *Summary.* All tested amines have high solubility water. Aqueous solutions of DAP and MAPA show strong negative deviations from Raoult's law in the whole range of amine concentrations.

The model for DAP may indicate a minimum azeotrope formation at high amine concentrations and below 313 K. No information to substantiate this has been found in the literature

**Table A4**Experimental (vapour + liquid) data for temperature T, pressure P, liquid-phase mole fraction x, and gas-phase mole fraction y, for 1,3-diaminopropane/DAP(1) + H<sub>2</sub>O(2)\*.

T/K	P/kPa	x <sub>1</sub>	u(x <sub>1</sub> )	y <sub>1</sub>	u(y <sub>1</sub> )	T/K	P/kPa	x <sub>1</sub>	u(x <sub>1</sub> )	y <sub>1</sub>	u(y <sub>1</sub> )	T/K	P/kPa	x <sub>1</sub>	u(x <sub>1</sub> )	y <sub>1</sub>	u(y <sub>1</sub> )
343.2	8.3	0.8134	0.008	0.7741	0.0080	353.2	13.3	0.8127	0.008	0.7009	0.0080	373.2	31.5	0.8006	0.008	0.6753	0.0080
343.1	9.7	0.5699	0.008	0.4174	0.0080	353.3	15.7	0.5739	0.008	0.3969	0.0080	373.2	38.2	0.5694	0.008	0.3799	0.0080
343.2	11.5	0.4309	0.008	0.2145	0.0080	353.2	18.5	0.4368	0.008	0.2263	0.0080	373.2	44.8	0.4270	0.008	0.2328	0.0080
343.3	13.7	0.3448	0.008	0.1082	0.0060	353.2	22.0	0.3456	0.008	0.1151	0.0060	373.2	51.9	0.3480	0.008	0.1175	0.0060
343.3	16.5	0.2773	0.008	0.0521	0.0040	353.3	25.5	0.2866	0.008	0.0607	0.0040	373.2	59.1	0.2810	0.008	0.0693	0.0040
343.2	18.6	0.2322	0.008	0.0333	0.0030	353.2	28.7	0.2389	0.008	0.0369	0.0030	373.2	65.2	0.2393	0.008	0.0397	0.0030
343.2	20.6	0.2001	0.008	0.0167	0.0015	353.3	31.9	0.2011	0.008	0.0199	0.0015	373.2	71.2	0.2002	0.008	0.0246	0.0020
343.2	22.4	0.1683	0.007	0.0106	0.0010	353.2	34.5	0.1707	0.007	0.0123	0.0010	373.2	76.0	0.1662	0.007	0.0169	0.0015
343.2	23.8	0.1483	0.007	0.0073	0.0007	353.2	36.7	0.1481	0.007	0.0081	0.0007	373.2	80.1	0.1479	0.007	0.0117	0.0011
343.2	25.1	0.1276	0.006	0.0046	0.0004	353.2	38.5	0.1299	0.006	0.0056	0.0004	373.2	83.2	0.1289	0.006	0.0093	0.0009
343.2	26.0	0.1126	0.006	0.0035	0.0003	353.2	39.9	0.1126	0.006	0.0044	0.0003	373.2	85.7	0.1167	0.006	0.0072	0.0007
343.2	26.8	0.1011	0.006	0.0025	0.0002	353.2	41.0	0.0986	0.006	0.0034	0.0002	373.1	87.7	0.1023	0.006	0.0071	0.0007
343.2	27.4	0.0887	0.005	0.0022	0.0002	353.2	42.0	0.0869	0.005	0.0024	0.0002	373.2	89.9	0.0914	0.005	0.0045	0.0005
343.2	27.9	0.0807	0.005	0.0018	0.0002	353.2	42.8	0.0760	0.005	0.0019	0.0002	373.2	91.2	0.0806	0.005	0.0035	0.0004
343.2	28.4	0.0733	0.005	0.0015	0.0002	353.2	43.4	0.0680	0.005	0.0015	0.0002	373.1	92.4	0.0719	0.005	0.0030	0.0003
343.2	28.6	0.0642	0.005	0.0013	0.0001	353.2	44.0	0.0603	0.005	0.0015	0.0001	373.2	93.8	0.0627	0.005	0.0026	0.0003
343.3	29.0	0.0576	0.004	0.0010	0.0001	353.2	44.4	0.0534	0.004	0.0012	0.0001	373.2	94.5	0.0570	0.004	0.0023	0.0002
343.2	29.3	0.0517	0.004	0.0009	0.0001	353.2	44.7	0.0476	0.004	0.0012	0.0001	373.2	95.3	0.0510	0.004	0.0020	0.0002
343.2	29.5	0.0464	0.004	0.0009	0.0001	353.2	45.0	0.0435	0.004	0.0009	0.0001	373.2	95.8	0.0463	0.004	0.0017	0.0002
343.3	29.7	0.0408	0.004	0.0008	0.0001	353.2	45.3	0.0384	0.004	0.0008	0.0001	373.2	96.5	0.0420	0.004	0.0014	0.0002

\* Standard uncertainties u are u(T) = 0.1 K; u(P) = 0.25 kPa. Data in italics are previously published in anonymized form in Trollebo et al. [3].

**Table A5**Experimental (vapour + liquid) data for temperature T, pressure P, liquid-phase mole fraction x, and gas-phase mole fraction y, for 2-(Isopropylamino)ethanol/IPAE(1) + H<sub>2</sub>O(2)\*.

T/K	P/kPa	x <sub>1</sub>	u(x <sub>1</sub> )	y <sub>1</sub>	u(y <sub>1</sub> )	T/K	P/kPa	x <sub>1</sub>	u(x <sub>1</sub> )	y <sub>1</sub>	u(y <sub>1</sub> )	T/K	P/kPa	x <sub>1</sub>	u(x <sub>1</sub> )	y <sub>1</sub>	u(y <sub>1</sub> )
333.2	5.3	0.8306	0.02	0.0955	0.002	353.3	18.6	0.7116	0.02	0.0849	0.002	373.2	8.6	0.9690	0.02	0.7549	0.007
333.2	5.5	0.8388	0.02	0.0961	0.002	353.2	22.4	0.6681	0.02	0.0690	0.002	373.2	10.6	0.9657	0.02	0.6100	0.006
333.3	5.6	0.8020	0.02	0.0925	0.002	353.2	25.4	0.6536	0.02	0.0525	0.002	373.2	36.7	0.7897	0.02	0.1279	0.002
333.2	5.7	0.8342	0.02	0.0963	0.002	353.2	27.7	0.6059	0.02	0.0450	0.002	373.2	51.8	0.6879	0.02	0.0777	0.002
333.3	7.9	0.7534	0.02	0.0566	0.002	353.2	26.4	0.6263	0.02	0.0523	0.002	373.2	67.9	0.5922	0.02	0.0520	0.002
333.2	9.8	0.6820	0.02	0.0419	0.002	353.2	29.3	0.6082	0.02	0.0440	0.002	373.2	81.1	0.4353	0.02	0.0350	0.002
333.3	12.0	0.5333	0.02	0.0300	0.002	353.2	35.8	0.4618	0.02	0.0284	0.002	373.2	87.6	0.3422	0.02	0.0277	0.002
333.2	15.0	0.4376	0.02	0.0180	0.002	353.2	39.1	0.3584	0.02	0.0219	0.002	373.2	91.4	0.2662	0.02	0.0237	0.002
333.2	16.5	0.3343	0.02	0.0141	0.0018	353.2	41.2	0.2978	0.02	0.0184	0.002	373.2	93.8	0.2173	0.02	0.0209	0.002
333.2	17.3	0.2697	0.02	0.0112	0.0013	353.3	42.7	0.2415	0.02	0.0166	0.0018	373.2	95.3	0.1842	0.02	0.0195	0.002
333.2	17.9	0.2205	0.02	0.0099	0.0010	353.2	43.5	0.2050	0.02	0.0145	0.0018	373.2	96.4	0.1561	0.02	0.0185	0.002
333.2	18.3	0.1863	0.02	0.0092	0.0010	353.2	44.2	0.1729	0.02	0.0130	0.0013	373.2	97.2	0.1348	0.018	0.0172	0.0017
333.2	18.5	0.1609	0.02	0.0081	0.0008	353.2	44.7	0.1503	0.02	0.0119	0.0010	373.2	97.8	0.1176	0.016	0.0167	0.0017
333.2	18.7	0.1400	0.018	0.0074	0.0007	353.2	45.0	0.1318	0.018	0.0113	0.0010	373.2	98.2	0.1016	0.015	0.0154	0.0015
333.3	18.9	0.1202	0.016	0.0070	0.0007	353.2	45.3	0.1153	0.016	0.0110	0.0010	373.2	98.5	0.0880	0.014	0.0145	0.0015
333.3	19.0	0.1046	0.015	0.0068	0.0007	353.2	45.5	0.1018	0.015	0.0109	0.0010	373.2	98.8	0.0775	0.012	0.0141	0.0014
333.3	19.1	0.0921	0.014	0.0062	0.0006	353.2	45.7	0.0900	0.014	0.0097	0.0010	373.2	99.3	0.0615	0.010	0.0129	0.0013
333.3	19.2	0.0830	0.013	0.0060	0.0006	353.2	45.9	0.0808	0.013	0.0093	0.0009	373.2	99.5	0.0551	0.010	0.0121	0.0012
333.2	19.2	0.0742	0.012	0.0056	0.0006	353.3	46.1	0.0723	0.012	0.0091	0.0009	373.2	99.7	0.0497	0.009	0.0117	0.0012
333.3	19.3	0.0664	0.010	0.0054	0.0005	353.3	46.2	0.0644	0.010	0.0090	0.0009	373.2	99.8	0.0442	0.008	0.0116	0.0012
333.2	19.3	0.0598	0.010	0.0052	0.0005	353.2	46.3	0.0578	0.010	0.0083	0.0008	373.2	100	0.0399	0.008	0.0111	0.0011
333.2	19.4	0.0540	0.009	0.0049	0.0005	353.3	46.4	0.0523	0.009	0.0081	0.0008	-	-	-	-	-	-
333.2	19.4	0.0442	0.008	0.0046	0.0005	353.2	46.4	0.0470	0.008	0.0077	0.0008	-	-	-	-	-	-
333.3	19.5	0.0399	0.008	0.0044	0.0005	-	-	-	-	-	-	-	-	-	-	-	-

\* Standard uncertainties u are u(T) = 0.1 K; u(P) = 0.25 kPa.

Since the possible azeotropic point of DAP is lying in the high concentration range, outside the practical range for an absorption process, it may seem of less industrial interest. However, situations can occur, when considering aerosol formation in the absorber and water wash systems, where evaporation of water and condensation of amine on the aerosol droplets can lead to very high amine concentrations. Examples of such behavior are given in Majeed et al. [37–40].

Aqueous solutions of IPAE and N-TBDEA show positive deviations from Raoult's law in the whole range of amine concentrations. N-TBDEA show especially strong deviations from Raoult's law. These solutions seem to have very high amine activity coefficients at infinite dilution. For IPAE the activity coefficients increase slightly with temperature. The activity coefficients of N-TBDEA are much higher than for IPAE and are also predicted to increase with temperature.

## 5. Conclusions

This paper presents new experimental data and modelling results for four amines. All have potential as new solvents for post combustion CO<sub>2</sub> capture. Both pure component data and data for amine-water solutions, based on ebulliometer measurements, are presented. The data were fitted to an Antoine equation and an NRTL model in two ways, first a combined fit of both pure component and binary data and then a separate fit to the data sets.

For MAPA, a relatively volatile amine, and with many both pure component and binary PTxy data points covering the whole temperature and concentration region of interest, the two procedures gave very similar results.

For DAP, also a relatively volatile amine, and with a large number of binary PTxy data points and sufficient pure component data covering the whole range of temperatures, the two methods gave

**Table A6**Experimental (vapour + liquid) data for temperature T, pressure P and liquid-phase mole fraction x, for N-*tert*-Butyldiethanolamine/N-TBDEA(1) + H<sub>2</sub>O(2)\*.

T/K	P/kPa	x <sub>1</sub>	u(x <sub>1</sub> )	T/K	P/kPa	x <sub>1</sub>	u(x <sub>1</sub> )	T/K	P/kPa	x <sub>1</sub>	u(x <sub>1</sub> )	T/K	P/kPa	x <sub>1</sub>	u(x <sub>1</sub> )
323.2	10.0	0.4142	0.008	333.2	18.0	0.2486	0.005	353.2	32.9	0.5779	0.01	373.2	68.3	0.6077	0.012
323.1	10.6	0.3602	0.007	333.2	19.2	0.1675	0.005	353.2	38.3	0.4151	0.008	373.2	94.0	0.2730	0.006
323.2	11.2	0.2191	0.005	333.2	19.5	0.1041	0.005	353.2	43.6	0.2749	0.006	373.2	95.9	0.2330	0.005
323.2	11.7	0.1285	0.005	333.2	19.4	0.1206	0.005	353.2	44.5	0.2403	0.005	373.2	98.0	0.1698	0.005
323.2	11.9	0.0964	0.005	333.2	19.6	0.1005	0.005	353.2	45.8	0.1701	0.005	373.2	99.2	0.1079	0.005
323.2	12.0	0.0667	0.005	333.2	19.6	0.0803	0.005	353.2	46.4	0.1199	0.005	373.2	85.0	0.4012	0.005
323.2	12.1	0.0495	0.005	333.2	19.7	0.0558	0.005	353.2	46.6	0.1038	0.005	373.2	89.9	0.3369	0.005
323.2	12.2	0.0363	0.005	333.2	19.8	0.0390	0.005	353.2	46.6	0.1005	0.005	373.2	98.7	0.1732	0.005
323.1	12.3	0.0270	0.004	333.1	16.5	0.4023	0.005	353.2	46.7	0.0791	0.005	373.2	99.3	0.1150	0.005
323.2	12.3	0.0205	0.004	333.1	17.5	0.3270	0.005	353.2	46.8	0.0565	0.005	373.2	99.7	0.0801	0.005
				333.2	19.1	0.1827	0.005	353.2	46.9	0.0388	0.005	373.2	99.9	0.0560	0.005
				332.7	19.5	0.1121	0.005	353.2	40.0	0.4154	0.005	373.2	100.1	0.0423	0.005
				332.8	19.6	0.0755	0.005	353.2	42.1	0.3475	0.005	373.2	100.1	0.0243	0.004
				332.9	19.7	0.0326	0.005	353.2	45.6	0.1761	0.005				
				333.0	19.8	0.0250	0.004	353.2	46.4	0.1127	0.005				
				333.0	19.8	0.0191	0.004	353.2	46.5	0.0755	0.005				
				333.0	19.8	0.0151	0.004	353.2	46.7	0.0550	0.005				
				333.0	19.8	0.0121	0.004	353.2	46.9	0.0411	0.005				
				333.1	19.9	0.0075	0.004	353.2	46.9	0.0302	0.005				
				333.1	19.9	0.0095	0.004	353.2	46.9	0.0229	0.004				
							0.005	353.2	47.0	0.0179	0.004				
							0.005	353.2	47.1	0.0140	0.004				

\* Standard uncertainties u are u(T) = 0.1 K; u(P) = 0.25 kPa. Data in italics are previously published in anonymized form in Trollebø et al. [3].

similar AARDs for both the binary and pure component fits. The standard deviations on the parameters were larger than the parameters for both procedures indicating that more data, in particular binary data, are needed.

With IPAE, a less volatile amine, limited pure component data were available and some discrepancies in the sets were found. However, the data cover a large temperature range. The binary PT<sub>xy</sub> data covered the whole composition range and most of the temperature range. In this case, the combined fit gave a good representation of both the pure component and binary data. However, the standard deviations on the parameters were large. The fit to separate data set resulted in an increase in the AARDs for both the pure component and binary data sets and large standard deviations in the parameters.

For N-TBDEA, an amine with low volatility, the data contained only pure component and binary PT<sub>x</sub> measurements. In this case, the two fitting procedures provided fits with similar AARDs.

For all amines, the best fits provided good to excellent representations of the available data.

### Declaration of Competing Interest

The authors declare that they have no known competing financial interests or personal relationships that could have appeared to influence the work reported in this paper.

### Acknowledgments

Financial support for this work by Aker Clean Carbon, EON, EnBW and the Norwegian Research Council CLIMIT program through the SOLVIT project, #189998, is greatly appreciated.

### Appendix A. Supplementary data

Supplementary data to this article can be found online at <https://doi.org/10.1016/j.jct.2019.105965>.

### References

[1] G.T. Rochelle, *Science* 325 (2009) 1652.

- V. Masson-Delmotte, P. Zhai, H.-O. Pörtner, D. Roberts, J. Skea, P.R. Shukla, A. Pirani, Moufouma-Okia, C. Péan, R. Pidcock, S. Connors, J.B.R. Matthews, Y. Chen, X. Zhou, M.I. Gomis, E. Lonnoy, Maycock, M. Tignor, and T. Waterfield (Eds.), IPCC, 2018: Summary for Policymakers. In: Global Warming of 1.5°C. An IPCC Special Report on the impacts of global warming of 1.5°C above pre-industrial levels and related global greenhouse gas emission pathways, in the context of strengthening the global response to the threat of climate change, sustainable development, and efforts to eradicate poverty, World Meteorological Organization, Geneva, Switzerland, 32 pp., 2018.
- A.A. Trollebø, M. Saeed, A. Hartono, I. Kim, H.F. Svendsen, *Energy Procedia* 37 (2013) 2066–2075.
- C.-P. Liao, R.B. Leron, M.-H. Li, *Fluid Phase Equilib.* 363 (2014) 180–188.
- X. Wang, K. Kang, W. Wang, Y. Tian, *J. Chem. Eng. Data* 58 (2013) 3430–3439.
- I.M.S. Lampreia, A.F.S. Santos, M.-L.C.J. Moita, L.C.S. Nobre, *J. Chem. Thermodyn.* 81 (2015) 167–176.
- M.A. Saleh, M.S. Ahmed, M.S. Islam, *Phys. Chem. Liq.* 40 (2002) 477–490.
- S.M. Islam, M.A. Saleh, *Phys. Chem. Liq.* 48 (2010) 156–170.
- T. Kimura, T. Ozaki, Y. Nakai, K. Takeda, S. Takagi, *J. Therm. Anal. Calorim.* 54 (1998) 285–296.
- T. Kimura, T. Kitai, T. Kamiyama, M. Fujisawa, *Thermochim. Acta* 450 (2006) 91–95.
- S. Mohren, A. Heintz, *Fluid Phase Equilib.* 133 (1997) 247–264.
- H.F. Svendsen, A.A. Trollebø, Amine absorbent and a method for CO<sub>2</sub> capture, Aker Engineering and Technology AS, USA, 2014.
- C. Antoine, *Comptes Rendus des Séances de l'Académie des Sciences*, 107 (681–684) 107 (1888) 778–780, 836–837.
- G.M. Wilson, *J. Am. Chem. Soc.* 86 (1964) 127–130.
- C.-C. Chen, L.B. Evans, *AIChE J.* 32 (1986) 444–454.
- H. Renon, J.M. Prausnitz, *AIChE J.* 14 (1968) 135–144.
- A. Hartono, E.O. Mba, H.F. Svendsen, *J. Chem. Eng. Data* 59 (2014) 1808–1816.
- F.G. Cottrell, *J. Am. Chem. Soc.* 41 (1919) 721–729.
- E.W. Washburn, J.W. Read, *J. Am. Chem. Soc.* 41 (1919) 729–741.
- I. Kim, H.F. Svendsen, E. Børresen, *J. Chem. Eng. Data* 53 (2008) 2521–2531.
- M. Rogalski, S. Malanowski, *Fluid Phase Equilib.* 5 (1980) 97–112.
- A. Hartono, M. Saeed, A.F. Ciftja, H.F. Svendsen, *Chem. Eng. Sci.* 91 (2013) 151–161.
- A. Hartono, F. Saleem, M.W. Arshad, M. Usman, H.F. Svendsen, *Chem. Eng. Sci.* 101 (2013) 401–411.
- J.D. Olson, *Fluid Phase Equilib.* 52 (1989) 209–218.
- T. Hertzberg, T. Mejdell. MODFIT for Matlab: parameter estimation in a general nonlinear multiresponse model, 1998.
- R.D. Chirico, M. Frenkel, J.W. Magee, V. Diky, C.D. Muzny, A.F. Kazakov, K. Kroenlein, I. Abdulagatov, G.R. Hardin, W.E. Acree, J.F. Brenneke, P.L. Brown, P. T. Cummings, T.W. de Loos, D.G. Friend, A.R.H. Goodwin, L.D. Hansen, W.M. Haynes, N. Koga, A. Mandelis, K.N. Marsh, P.M. Mathias, C. McCabe, J.P. O'Connell, A. Pádua, V. Rives, C. Schick, J.P.M. Trusler, S. Vyazovkin, R.D. Weir, J. Wu, *J. Chem. Eng. Data* 58 (2013) 2699–2716.
- Z. Bouzina, I. Mokbel, A. Negadi, J. Jose, L. Negadi, *J. Chem. Thermodyn.* 92 (2016) 43–54.
- S.P. Verevkin, Y. Chernyak, *J. Chem. Thermodyn.* 47 (2012) 328–334.
- C.L. Yaws, P.K. Narasimhan, C. Gabbula, Yaws' handbook of Antoine coefficients for vapour pressure, second Electronic Edition., Knovel, 2015.
- N.C.-B. Ahmed, L. Negadi, I. Mokbel, J. Jose, *J. Chem. Thermodyn.* 43 (2011) 719–724.



- [31] V.A. Pozdeev, S.P. Verevkin, *J. Chem. Thermodyn.* 43 (2011) 1791–1799.
- [32] K.A. Pividal, S.I. Sandler, *J. Chem. Eng. Data* 35 (1990) 53–60.
- [33] M. Fulem, K. Růžička, C. Červinka, A. Bazyleva, G. Della Gatta, *Fluid Phase Equilib.* 371 (2014) 93–105.
- [34] B.P. Soares, V. Štejfa, O. Ferreira, S.P. Pinho, K. Růžička, M. Fulem, *Fluid Phase Equilib.* 473 (2018) 245–254.
- [35] H.C. Van Ness, H.P. Isermann, *Pure Appl. Chem.* 67 (1995) 859–872.
- [36] J.M. Prausnitz, E.G.d. Azevedo, R.N. Lichtenthaler, *Molecular thermo-dynamics of fluid-phase equilibria* 07458, Prentice Hall PTR, Upper Saddle River, New Jersey, 1999.
- [37] H. Majeed, H. Knuutila, M. Hillestad, H.F. Svendsen, *Energy Procedia* 114 (2017) 977–986.
- [38] H. Majeed, H. Knuutila, M. Hillestad, H.F. Svendsen, *Int. J. Greenhouse Gas Control* 64 (2017) 212–222.
- [39] H. Majeed, H.K. Knuutila, M. Hillestad, H.F. Svendsen, *Int. J. Greenhouse Gas Control* 58 (2017) 114–126.
- [40] H. Majeed, H.F. Svendsen, *Chem. Eng. J.* 333 (2018) 636–648.

JCT 2019-156